

An Evaluation of GNSS code and phase solutions

F.Zarzoura^{1,2}, R. Ehigiator – Irughe^{1*}, M. O. Ehigiator^{3,2}

¹ Faculty of Engineering, Mansoura University, Egypt

² Siberian State Geodesy Academy, Department of Engineering Geodesy and GeoInformation Systems, Novosibirsk, Russia.

³ Faculty of Basic Science, Department of Physics and Energy, Benson- Idahosa University, Benin City, Nigeria.

¹fawzyhamed2011@yahoo.com, ^{*}raphehigiator@yahoo.com, ²geosystems_2004@yahoo.com

Abstract

Global Navigation satellite System (GNSS) has become an important tool in any endeavor where a quick measurement of geodetic position is required. GNSS observations contain both Systematic and Random errors. Differential GPS (DGPS) and Real Time Kinematic (RTK) are two different observation techniques that can be used to remove or reduce the errors effects arising in ordinary GNSS. This study has utilized procedure to compare DGPS with code and phase solutions.

Key words: GNSS, Code and Phase solution, RTK.

1.0 Introduction

Real time GPS applications are commonly based on the code (range) measurements. These measurements are affected by many biases, which cause the derived three-dimensional coordinates to be deviated, significantly, from the true positions [1]. Differential GPS (DGPS) is a method that can be used to remove or reduce the ionosphere, troposphere and orbit effects.

Differential GPS (DGPS) is a method that can be used to remove or reduce the ionosphere, troposphere and orbit effects. In DGPS, corrections are generated at a base station and then the rover receiver has the value of errors such as ionosphere, troposphere and satellite ephemeris errors. In addition, the satellite or receiver clock errors can also be cancelled out by differencing between two receivers or two satellites respectively. Therefore, DGPS can give high accuracy after the significant reduction of those errors.

DGPS works effectively in local areas within 50 kilometres. Therefore, conventional local area DGPS method can't give a reasonable accuracy for large area applications. The corrections at the user sites can enhance the carrier phase ambiguity resolution and improve the positioning accuracy in Real-Time Kinematics (RTK) situations.

1.2 Test Field Procedure:

A dual frequency GPS receiver of LEICA RTKGPS 1200 system, was setup at the reference point (NGN95), which serve as the control station (master) throughout the research. The receiver at the master station was on static mode and at observation rate of (5) seconds. The rover receiver of the same LEICA type was setup at point number (PM-08) that is about 3 km from the reference receiver with the same parameters as the master receiver as presented in figure (1) below. All other stations were similarly occupied as presented in figure (1) and table (1) below.

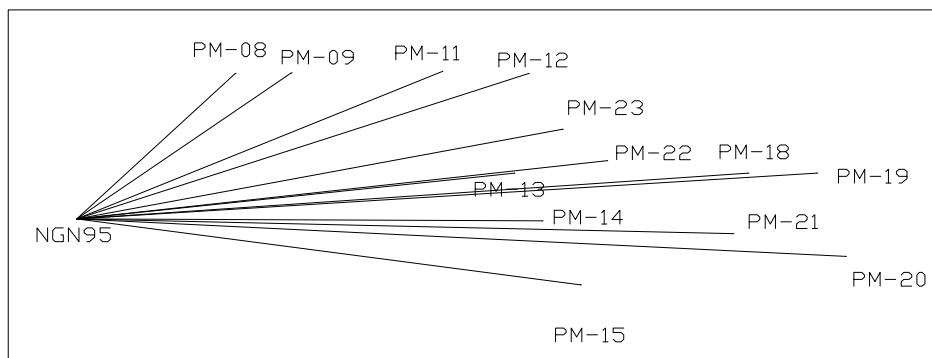


Figure 1: GPS observation

Table 1: schematic diagram of distance relationship.

NGN95	PM-08	PM-09	PM-11	PM-12	PM-13	PM-14	PM-15
Dis.,(m)	2920	3453	5119	6110	5601	5910	6467
NGN95	PM-17	PM-18	PM-19	PM-20	PM-21	PM-22	PM-23
Dis.,(m)	7516	8575	9416	9775	8330	6743	6222

In addition, the other essential observation operating parameters are the same for both reference and rover receivers, which are: the Health/L2 mode is selected as Auto, the minimum elevation angle (mask angle) is (10) degrees, the data rate (5) seconds, initialization period is (10) minutes and the minimum number of (4) satellites.

1.3 GPS Observation Equations

Two different models for the GPS observations can be applied: one model for the code measurements and the other model for phase measurements. The code observation is the difference between the transmission time of the signal from the satellite and the arrival time of that signal at the receiver multiplied by the speed of light [2]. The time difference is determined by comparing the replicated code with the received one. The time difference is the time shift essential to align these two codes. The code observation represents the geometric distance between the GPS satellite and the receiver plus the bias caused by the satellite and the receiver clock offsets. Moreover, the atmospheric bias and the noise influence the code observations [3].

The basic observation equation related to the code measurement of a receiver (a) to a satellite (j) can be written as [4].

$$R_a^j(t) = \rho_a^j(t) + C \delta^j(t) - C \delta_a(t) + \Delta_a^j Ion(t) + \Delta_a^j Trop(t) + \zeta \quad (1-1)$$

Where:

$R_a^j(t)$	The biased code geometric range
$\rho_a^j(t)$	The space distance between the satellite and receiver
C	Speed of light.
$\delta^j(t)$	The bias of the satellite clock .
$\delta_a(t)$	The bias of the receiver clock
$\Delta_a^j Ion(t)$	The ionosphere delay in m.
$\Delta_a^j Trop(t)$	The tropospheric delay in m.
ζ	The observation noise

The phase measurement is the difference between the generated carrier phase signal in the receiver and the received signal from the satellite. The phase measurement is in range units when it is multiplied by the signal wavelength. It represents the same range and biases as the code observation, and additionally the range related to the unknown integer ambiguities. The observation equation for the phase measurement can be written as the follows [4]:

$$\varphi_a^j(t) = \frac{1}{\lambda} \rho_a^j(t) + N_a^j + f \delta^j(t) - f \delta_a(t) - \frac{1}{\lambda} \Delta_a^j Ion(t) + \frac{1}{\lambda} \Delta_a^j Trop(t) + \varepsilon \quad (1-2)$$

Where:

$\varphi_a^j(t)$	The phase difference between the received code and the replica generated phase in receiver
N_a^j	The unknown integer ambiguity.
λ	The wavelength of the carrier wave.
f	The signal frequency.
ε	The phase observation noise.

1.4 Double-difference mode

The double-difference mode is executed between a pair of receivers and pair of satellites as shown in figure (2). Denoting the stations by a (a), (b) and the satellites involved by (j), (k). Two single-differences according to equation (1-3) can be applied [4]:

$$\left. \begin{aligned} \phi_{a,b}^j(t) &= \frac{1}{\lambda} \rho_{a,b}^j(t) + N_{a,b}^j - f^j \delta_b(t) \\ \phi_{a,b}^k(t) &= \frac{1}{\lambda} \rho_{a,b}^k(t) + N_{a,b}^k - f^k \delta_b(t) \end{aligned} \right\} \quad (1-3)$$

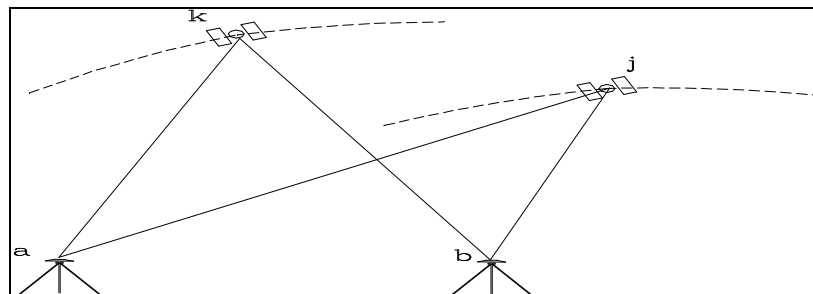


Figure 2: The double-difference technique.

These single-differences are subtracted to get the double - difference model as:

$$\phi_{a,b}^j(t) - \phi_{a,b}^k(t) = \frac{1}{\lambda} [\rho_{a,b}^j(t) - \rho_{a,b}^k(t)] + [N_{a,b}^j - N_{a,b}^k] \quad (1-4)$$

Using the short hand notation as in the single-difference

$$\phi_{a,b}^{j,k}(t) = \frac{1}{\lambda} \rho_{a,b}^{j,k}(t) + N_{a,b}^{j,k} \quad (1-5)$$

The result of this mode is the omission of the receiver clock offsets. The double-difference model for long baselines when there is a significant difference in the atmospheric effect between the two baselines ends can be expressed [2]:

$$\phi_{a,b}^{j,k}(t) = \frac{1}{\lambda} \rho_{a,b}^{j,k}(t) + N_{a,b}^{j,k} - \frac{1}{\lambda} \Delta_{a,b}^{j,k} Ion(t) + \frac{1}{\lambda} \Delta_{a,b}^{j,k} Trop(t) \quad (1-6)$$

1.5 Network Double-difference Error Observable

Assuming that a network of n GPS reference stations is available, the network single observable vector (l) is defined as follows:

$$l_n = \left[\bar{\phi}_l^l, \dots, \bar{\phi}_l^{n_{sv}}, \dots, \bar{\phi}_{n_{rx}}^l, \dots, \bar{\phi}_{n_{rx}}^{n_{sv}} \right]^T \quad (1-7)$$

Where $\bar{\phi}_{n_{rx}}^{n_{sv}}$ is the phase measurement minus true - range observable from receiver rx to satellite sv in single form.

The geometric ranges are calculated using precise coordinates of the reference stations. n_{rx} is the number of reference stations, and n_{sv} is the number of satellites observed at each station. The network double -difference observable vector is [2]:

$$\nabla \Delta l_n = \left[\nabla \Delta \bar{\phi}_{l_2}^{l_2}, \dots, \nabla \Delta \bar{\phi}_{l_2}^{n_{sv}}, \nabla \Delta \bar{\phi}_{l_3}^{l_2}, \dots, \nabla \Delta \bar{\phi}_{l_3}^{n_{sv}}, \dots, \nabla \Delta \bar{\phi}_{n_{rx}}^{l_2}, \dots, \nabla \Delta \bar{\phi}_{n_{rx}}^{n_{sv}} \right]^T \quad (1-8)$$

Where: $\nabla \Delta \bar{\phi}_{ab}^{xy}$ is the double - difference measurement minus true - range observable between receivers a, b and satellites x, y . mathematically, a double -difference matrix B can be used to relate the network single observables and the network double - difference observables such that:

$$\nabla \Delta l_n = B_n l_n \quad (1-9)$$

$$B_n = \frac{\partial \nabla \Delta l_n}{\partial l_n} \quad (1-10)$$

The dimension of the double - difference matrix is ($d_m \times m$), where d_m is the number of network double - difference observables and m is the number of network single observations [2]. For example, consider an example of 2 receivers a, b where each receiver tracks 3 satellites $1, 2, 3$.

The network single observable vector is: $\left[l_a^1, l_a^2, l_a^3, l_b^1, l_b^2, l_b^3 \right]$

Choosing satellite 1 to be the base satellite, the double - difference vector, is given as:

$$\left[\nabla \Delta l_{ab}^{12}, \nabla \Delta l_{ab}^{13} \right] = \left[(l_a^1 - l_b^1) - (l_a^2 - l_b^2), (l_a^1 - l_b^1) - (l_a^3 - l_b^3) \right] \quad (1-11)$$

Performing the partial derivative as shown in equation (1-12),

matrix B is: $B_n = \begin{bmatrix} 1 & -1 & 0 & -1 & 1 & 0 \\ 1 & 0 & -1 & -1 & 0 & 1 \end{bmatrix}$

If the double - difference ambiguities of network baselines are correctly resolved, the network double - difference error vector is:

$$\nabla\Delta\delta l_n = \nabla\Delta l_n - \lambda\nabla\Delta N_n = \nabla\Delta d_c\phi(p, p_0) + \nabla\Delta\delta_u\phi \quad (1-12)$$

Where: $\nabla\Delta d_c\phi(p, p_0)$ is the network double - difference spatially correlated errors and $\nabla\Delta\delta_u\phi$ represents the network double - difference uncorrelated errors. A Kalman filter is used to estimate the float ambiguities using L1 observations, L2 observations and stochastic modeling of the ionospheric error. The ratio test is used to validate the fixed ambiguities. The network double - difference errors are also called the estimated network double - difference corrections. These will be used as input measurements for the linear minimum error variance estimator.

2.2 Data Processing:

After collecting the field data, using dual frequency DGPS receivers, as mentioned above, both L1 data and L2 data becomes available. Consequently, to satisfy the objective of this research, the collected data was processed using LGO software. The run is performed using CODE and PHASE solution approach.

3.0 Results and analysis.

The main objective was to investigate the accuracy standard of the final resulted coordinates of surveyed points between Dual Frequency DGPS CODE ONLY solution, and CODE AND PHASE solution, for short distances (less than 10km). LGO software has the capability of producing results of these two different solutions.

Table 4.1 shows the output coordinates from the LGO software. Keeping in mind that, all these points ambiguity have been resolved.

The coordinate's discrepancies (ΔE , ΔN), and positional discrepancies (ΔP), between the two dual frequency DGPS solutions, of CODE ONLY, and CODE AND PHASE, data processing, are evaluated in the following manner:

$$\begin{aligned} \Delta E &= E_{\text{code only}} - E_{\text{code and phase}} \\ \Delta N &= N_{\text{code only}} - N_{\text{code and phase}} \\ \Delta P &= \sqrt{\Delta E^2 + \Delta N^2} \end{aligned}$$

Where, the CODE AND PHASE solution is assumed to be the standard or reference solution. Table (4.2) includes such discrepancies, for the all fourteen points under consideration, including the reference point (NGN95). In addition, figure (4.3) displays the variations of coordinates discrepancies, (ΔE , ΔN , ΔP), as computed at each point, and defined by the point ID.

Table 4.1: LGO software, CODE AND PHASE and CODE ONLY results

Pt. Id	Code + Phase Solution		Code Solution	
	East	North	East	North
NGN95	234604.403	3180412.773	234604.403	3180412.773
PM-08	236618.466	3182526.913	236618.788	3182527.345
PM-09	237328.137	3182535.806	237328.648	3182536.36
PM-11	239251.862	3182558.970	239251.092	3182559.462
PM-12	240337.101	3182527.901	240337.722	3182527.071
PM-13	240165.606	3181077.388	240166.069	3181077.831
PM-14	240514.765	3180383.594	240513.924	3180382.693
PM-15	240999.488	3179448.527	241000.228	3179448.957
PM-17	241931.228	3182088.399	241930.368	3182087.469
PM-18	243123.530	3181387.700	243123.885	3181387.058
PM-19	243996.530	3181079.872	243997.201	3181078.962
PM-20	244364.367	3179864.487	244364.799	3179864.958
PM-21	242934.016	3180318.405	242934.648	3180317.693
PM-22	241343.872	3180193.391	241344.193	3180193.805

Table 4.2: Discrepancies between CODE AND PHASE and CODE ONLY solutions

Pt. Id	$\Delta E(m)$	$\Delta N (m)$	ΔP	Comments
NGN95	0	0	0	Control
PM-08	0.322	0.432	0.539	
PM-09	0.511	0.554	0.754	
PM-11	-0.77	0.492	0.914	
PM-12	0.621	-0.83	1.036	
PM-13	0.463	0.443	0.641	
PM-14	-0.841	-0.901	1.23	

PM-15	0.74	0.43	0.856	
PM-17	-0.86	-0.93	1.267	
PM-18	0.355	-0.642	0.734	
PM-19	0.671	-0.91	1.131	
PM-20	0.432	0.471	0.639	
PM-21	0.632	-0.712	0.952	
PM-22	0.321	0.414	0.524	

In order to visualize the range of discrepancies variations, the corresponding statistical parameters (Maximum, Minimum, Mean, and STDV for single determination) are computed for the 2-D coordinates discrepancies, (ΔE , ΔN), as well as for the positional discrepancies, (ΔP), and summarized in table (4.3).

From table (4.3) and figure (4.3) one can see that all resulted discrepancies are fluctuating round the zero value, in both positive and negative directions, with some values showing relatively large discrepancies.

From table (4.3), for instance, as an example, the positional discrepancies, (ΔP), are varying between zero, 1.267, with mean value of 0.843, and STDV of 0.253 for single determination. Similar statements can be stated for the other evaluated discrepancies, (ΔE), and (ΔN).

Table (4.3): Maximum, minimum and standard deviation with the above differences

	$\Delta E(m)$	$\Delta N(m)$	$\Delta P(m)$
STDV.	0.604	0.655	0.253
Max.	0.74	0.554	0
Min.	-0.86	-0.93	1.267

Moreover, from figure (4.3) one can easily find points of relatively large discrepancies.

Of course, one should expect undesirable observing circumstances at such points, particularly, the number of available satellites, and consequently, the resulted GDOP value.

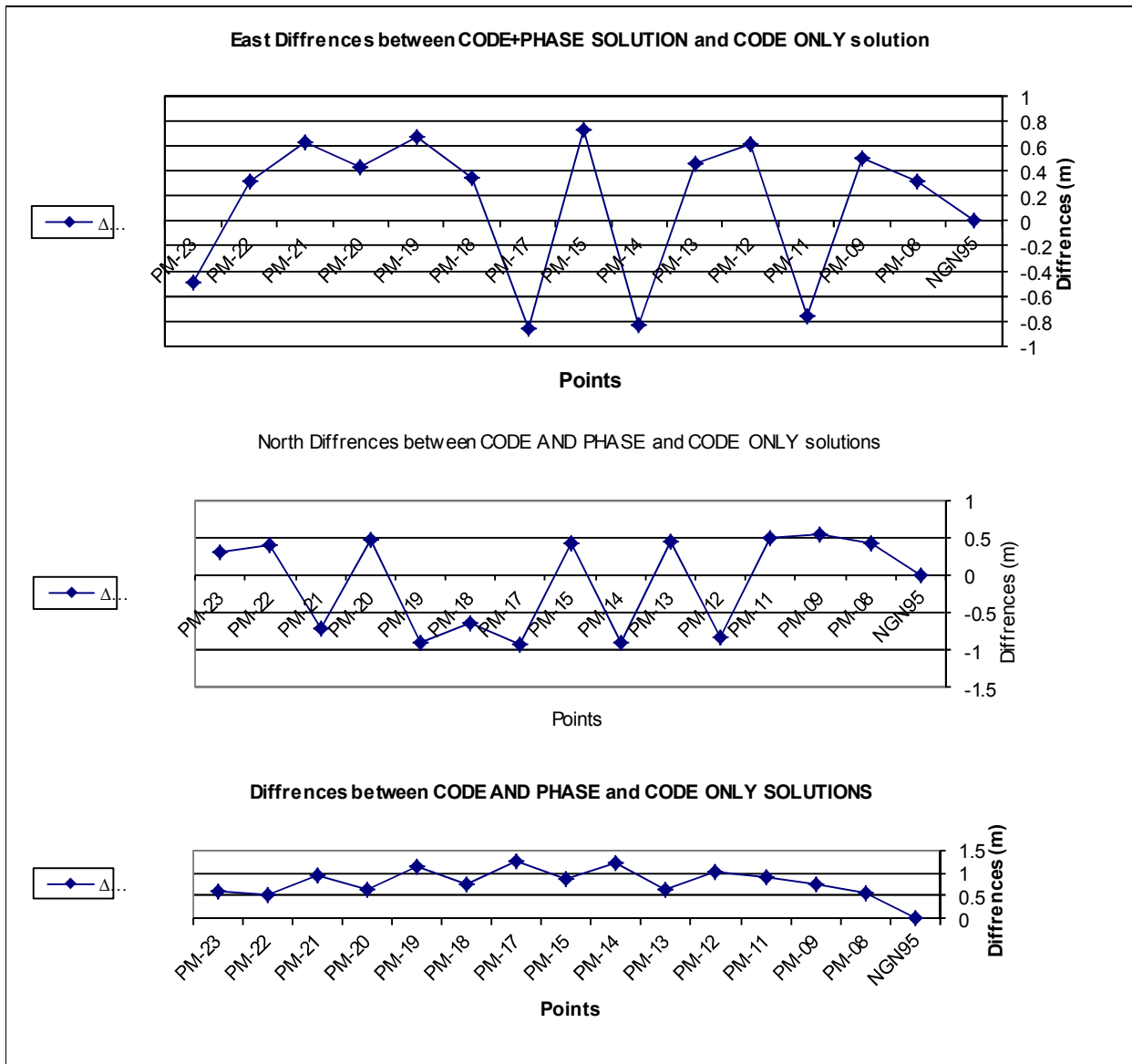


Figure 3 - Variations between CODE AND PHASE and CODE ONLY solutions

REFERENCES

1. F. Zarzoura (2008) Accuracy study of wide area GPS networks MSc thesis department of public work Mansoura University Egypt.
2. Elghazoly.A , (2005) "Accuracy Aspects of Static GPS With Special Regard to Internet- Aided Techniques "Faculty of engineering ,Alexandria. Egypt.
3. Enge, P.K., and Van Dierendonck, A.J.,(1995) "Wide Area Augmentation System, in Global Positioning System": Theory and Applications, Vol. II, ed. B.W.
4. Hofmann-Wellenhof, B., Lichtenegger, H. & Collins, J., 2001 GPS: Theory & Practice. Springer-Verlag, Vienna New York, 5th ed.
5. Ehigiator – Irughe, R. O.M. Ehigiator and S. A. Uzoekwe (2011)

Establishment of Geodetic Control in Jebba Dam using CSRS – PPP Processing software Journal of Emerging Trends in Engineering and Applied Sciences (JETEAS) 2 (5): pp. 763-769 Scholarlink Research Institute Journals.
6. Vladimir A. Seredovich, Ehigiator – Irughe, R. and Ehigiator, M.O.(2012)

PPP Application for estimation of precise point coordinates – case study a reference station in Nigeria Paper published at Federation International Geodesy (FIG) Rome Italy 6th – 12th May, 2012.
7. Ehigiator – Irughe, R. Nzodinma, V.N. and Ehigiator, M.O. (2012)

An Evaluation of Precise point positioning (PPP) in Nigeria using ZVS3003 Geodetic Control as a case study” Research Journal of Engineering and Applied Sciences (RJEAS) 1 (2) pp.102 - 109. A United State Academy publications USA.

About authors, visit: www.geosystems2004.com